Relative Magnitude of Gaussian Curvature Using Neural Network and Object Rotation of Two Degrees of Freedom

Yi Ding[1]   Yuji Iwahori[2]   Tsuyoshi Nakamura[1]   Lifeng He[3] Robert J.Woodham[4] Hidenori Itoh[1]

[1] Nagoya Institute of Technology
[3] Aichi Pref. University

[2] Chubu University
[4] University of British Columbia

Abstract

We propose a new approach to recover the relative magnitude of Gaussian curvature from multiple images. Previous approaches recover the sign of Gaussian curvature from the spatial relationship of points mapped onto a sphere. Here, the relative magnitude of Gaussian curvature is recovered at each point. No calibration object is required. Instead, the test object itself is rotated in both the vertical and horizontal directions to estimate the position coordinates of a marker point. An RBF neural network learns the mapping of intensities to marker position coordinates along a virtual sphere. That is, self-calibration is performed by moving a marker point. The neural network represents the mapping of observed image intensities to coordinates on a virtual sphere. Self-calibration makes it possible then to recover the relative magnitude of Gaussian curvature at each point. Experiments on real data are demonstrated.

1. Introduction

Surface curvature is useful to describe the structure of an object surface. The Gaussian curvature at a point on a surface is viewpoint invariant, making it useful for object recognition and shape recovery in the computer vision.

In a previous approach, Woodham [1] proposed a method to recover local surface orientation and surface curvature using photometric stereo. Photometric stereo uses multiple images of a test object taken from a fixed viewpoint under different conditions of illumination.

Iwahori, Woodham *et al.* [2] [3] pursued neural network implementations of photometric stereo. A neural network replaces an explicit LUT (lookup table) as a way to do non-parametric functional approximation.

Angelopoulou and Wolf [4] and Okatani and Deguchi [5] recover the sign of Gaussian curvature from three images acquired under different illumination conditions. The values of the surface gradient and the light source directions themselves are not known explicitly. These methods are applicable to diffuse reflectance.

Iwahori *et al.* [6] [7] proposed a method to recover the relative magnitude of Gaussian curvature using an RBF neural network. Local classification of surface curvature also is provided.

Previous approaches either used a calibration sphere with the same reflectance properties as the test object or assumed diffuse (i.e., Lambertian) reflectance. A cali-

bration sphere also can be used as a learning object for a neural network. Calibration methods require that images of a test object and the calibration sphere be acquired under the same illumination conditions.

In this paper, we propose a new method to recover the relative magnitude of Gaussian curvature from the test object itself without using a calibration sphere. Except that one of the light source directions is aligned with the viewing direction, no explicit assumptions need to be made either about light source directions or about the functional model of surface reflectance.

Two degree of freedom rotation of the test object itself generates the neural network learning data. Four light sources and hence four images are used to recover the relative magnitude of the Gaussian curvature of a test object, including a possibly varying color reflectance factor.

2. Principle

2.1. Empirical constraint

As originally defined, photometric stereo determines the local surface normal vector from observed image irradiances. Empirical photometric stereo uses a calibration object of known shape with the same reflectance properties as the test object. Under orthographic projection and distant (i.e., parallel) light sources, three images from three different light source directions are sufficient also to determine the surface curvature.

Let the image irradiances at (x_{obj}, y_{obj}) on the test object be $(e_{1obj}, e_{2obj}, e_{3obj})$, and at (x_{sph}, y_{sph}) on the calibration sphere be $(e_{1sph}, e_{2sph}, e_{3sph})$. Under the assumption that the reflectance characteristics of the test object and the calibration sphere are the same, the following constraint

$$\begin{cases} e_{1obj}(x_{obj}, y_{obj}) = e_{1sph}(x_{sph}, y_{sph}) \\ e_{2obj}(x_{obj}, y_{obj}) = e_{2sph}(x_{sph}, y_{sph}) \\ e_{3obj}(x_{obj}, y_{obj}) = e_{3sph}(x_{sph}, y_{sph}) \end{cases} \qquad (1)$$

is satisfied when the surface normal at the test object point is the same as that at the point on the calibration sphere. The mapping of points on the test object to the sphere is key to the recovery of surface curvature.

2.2. Gaussian curvature and sign

An RBF neural network realizes non-parametric functional approximation in multi-dimensional spaces. Here, an RBF neural network learns the mapping of (e_1, e_2, e_3) to (x_{sph}, y_{sph}) for each point on a sphere. The resulting network generalizes in that it predicts a point (x_{sph}, y_{sph}) on the sphere, given any input value (e_1, e_2, e_3). The resulting NN outputs the corresponding (x_{sph}, y_{sph}) on the sphere for each input (e_1, e_2, e_3) from points on the test object.

The two principal curvatures, k_1 and k_2 are used to characterize the local shape of the surface. These are the maximum and minimum local curvatures, respectively. The signs of the two principal curvatures classify surfaces into six local surface shape classes (Table 1).

Table 1. Relation between surface shape classes and principal curvatures.

	$k_2 > 0$	$k_2 = 0$	$k_2 < 0$
$k_1 > 0$	convex	convex parabolic	hyperbolic
$k_1 = 0$		plane	concave parabolic
$k_1 < 0$			concave

The signs of the principal curvatures defines six local surface shape classes: convex, concave, convex parabolic, concave parabolic, hyperbolic, and plane. When we take four local points that surround a point of interest on a test object, we can investigate how these points are mapped onto a sphere. The ordering of these mapped points (x_{sph}, y_{sph}) on the sphere can be used to recover the Gaussian curvature and to classify the local surface according to the six classes given in Table 1.

2.3. Magnitude of Gaussian curvature

The local surface curvature class can be determined from multiple images. The magnitude of the Gaussian curvature provides additional information. The magnitude of the Gaussian curvature can be either absolute or relative. Absolute values of the Gaussian curvature typically are very small. A relative value can be more useful to characterize local surface features. The principle used to recover a relative magnitude of the Gaussian curvature is as follows:

Consider the position coordinates (x_{sph}, y_{sph}) of four local points mapped onto a sphere. Calculate the area on the sphere defined by the four mapped points. The ratio of this area to the corresponding area in the image defines a relative magnitude of the Gaussian curvature.

For a standard configuration of four local image points, the corresponding area on the sphere is used as the relative magnitude of the Gaussian curvature. A more detailed description of how to recover relative magnitude of Gaussian curvature for a test object using a calibration sphere is given in [7], which shows results for test objects with uniform albedo.

3. Self-Calibration with two DOF rotations

3.1. Non-Uniform Albedo

Let j be the j-th light source. Let the y-axis be the vertical direction and let the x-axis be the horizontal direction. Here, $e_j(x, y)$ is the image irradiance and $R_j(n_x, n_y, n_z)$ is the reflectance map of the test object, where (n_x, n_y, n_z) is the surface normal at image point (x, y). For four light source photometric stereo under the orthographic projection, the following image irradiance equations hold:

$$\begin{cases} e_1(x, y) = \rho(x, y) R_1(n_x, n_y, n_z) \\ e_2(x, y) = \rho(x, y) R_2(n_x, n_y, n_z) \\ e_3(x, y) = \rho(x, y) R_3(n_x, n_y, n_z) \\ e_4(x, y) = \rho(x, y) R_4(n_x, n_y, n_z) \end{cases} \quad (2)$$

where $\rho(x, y)$ is the albedo at point (x, y). From equations (2), ρ can be eliminated as follows:

$$e_j'(x, y) = \frac{e_j(x, y)}{\sqrt{e_1(x, y)^2 + e_2(x, y)^2 + e_3(x, y)^2 + e_4(x, y)^2}}$$

(for $j = 1, 2, 3, 4$)   (3)

The objective now is to determine the mapping of (e_1', e_2', e_3', e_4') to (n_x, n_y, n_z) using only the test object itself.

3.2. Rotation of the test object

The novel idea in this paper is to obtain the training data for a neural network from the target object itself. Training data are obtained from point correspondences of a distinct marker point when the object undergoes a known rotation. During rotation, test object image irradiance $e_j(x, y)$ is acquired for each light source j.

Suppose the test object is rotated along the horizontal axis (x-axis) and along the vertical axis (y-axis) with known step. In particular, suppose the test object is rotated in 5 degree steps from −90 degrees to +90 degrees along the horizontal axis and along the vertical axis. Images are acquired under each of four light sources. Figure 1 illustrates.

Let r be the distance between the marker point and the rotation axis. Then, r is the radius of rotation. The test object is rotated in a fixed pattern and, with simple geometric calculation, the training set for neural network is obtained from the image irradiances of the marker point.

Figure 1. Two DOF Self-Calibration

For each fixed vertical direction of the marker point, the test object is rotated in 5 degree steps in the horizontal direction from −90 degrees to +90 degrees. This movement is repeated by changing the vertical direction in 5 degree steps from −90 degrees to +90 degrees.

The Cartesian coordinates (x, y) of the marker point are represented in terms of the radius r and spherical coordinates, the azimuth angle a and the zenith angle b as follows:

$$x = r \times \cos b \times \sin a$$
$$y = r \times \sin b \qquad (4)$$

To calibrate the starting position, the position of the marker point (x, y) can be calculated from the radius r and rotation angle (a, b). The starting position is calibrated at vertical direction 0 degrees and horizontal direction 0 degrees.

The radius r is estimated from an equilateral triangle using the position (x_{-30}, y_0) in the horizontal direction at −30 degrees and the position (x_{30}, y_0) in the horizontal direction at 30 degrees as

$$r = x_{30} - x_{-30} \qquad (5)$$

3.3. Neural network learning

Four light sources are used so that four input images are acquired for each object pose. To calibrate the initial marker point, one light source direction is chosen to be aligned with the viewing direction, i.e., the direction towards the camera. When the surface normal at the marker point (x, y) points towards the camera and the light source, the image irradiance of the marker point becomes locally brightest. For the starting position, the surface normal at the marker point is required to point towards the camera.

Under orthographic projection, the position of the marker is estimated from Equations (4) and (5). For each position of the marker point, the irradiance in each image $e_j(x, y)$ is obtained and the resulting set of positions and image irradiances is used for neural network learning. It is possible that observed image irradiances and the corresponding point coordinates (x, y) may include some unexpected data such as cast shadow. Such data are removed prior to neural network learning.

Since the original data contains noise, it is better to obtain smooth data for $e'_j(x, y)$. To smooth image irradiance, a neural network learns the mapping of $e'_j(x, y)$ to $e'_j(x, y)$. An RBF neural network is used to learn input/output data obtained from the marker point at each pose of the object. The result predicts irradiance $e'_j(x_{obj}, y_{obj})$, given any input point (x_{obj}, y_{obj}). The structure of this neural network is shown in Figure 2.
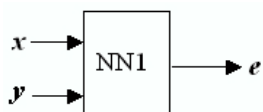

Figure 2. Neural network to obtain smooth e'_j

The neural network generalizes its output with nonlinear multi-dimensional interpolation. In the learning during self-calibration, the albedo effect is removed using Equa-

tion (1) and the normalized e'_j are given as the input to the neural network. The learning of the mapping of e'_j to (x, y) is also done using an RBF neural network. The resulting neural network estimates the position (x, y) on a virtual sphere.
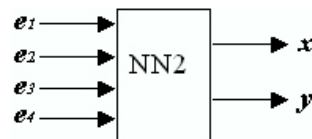

Figure 3. Neural network to estimate Gaussian curvature

The four mapped coordinates (x, y) obtained for the four local neighboring points on the object are used to recover not only the local surface curvature class but also the relative magnitude of the Gaussian curvature at each point.
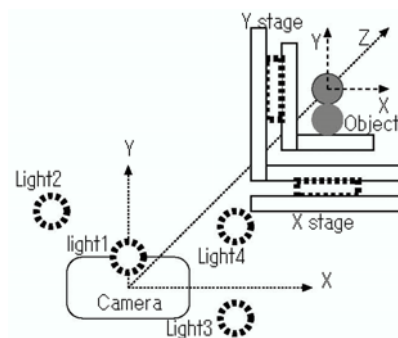
4. Experiments

4.1. Environment

Figure 4. Experimental environment

Figure 4 illustrates our experimental environment. The test object is placed on the rotation table as shown in Fig.1. Four light sources are used to illuminate the test object. One light source is aligned with the viewing direction. Four images are obtained under four different illuminations for each object pose during rotation. The test object is rotated every 5 degrees between −90 degrees and +90 degrees. The total number of poses under rotation is 37×37. Thus, a total of 37×37×4 images are taken to perform the self-calibration.

4.2. Results

Views of the test object are shown in Figure 5-(a) and Figure 6-(a). To learn the mapping of (e'_1, e'_2, e'_3, e'_4) to (x, y), RBF neural network learning proceeded for 100 epochs.

The virtual sphere image generalized by the neural network of Fig.2 was 256 × 256 pixels. To learn the mapping of the neural network of Fig.3, sample points were taken every 4 dots apart. Sample points were taken every 2 dots apart from the 512 × 512 pixel test image. As a preprocessing smoothing step, the first NN in Fig.2 is used to get smooth data e_j.

Fig.5-(b) and Fig.6-(b) show the six local surface

classes: convex, concave, convex parabolic, concave parabolic, hyperbolic surfaces and plane. Fig.7 shows the curvature class encoding as gray values. Fig.5-(c) and Fig.6-(c) show the estimated relative magnitude of Gaussian curvature. Again, the result is encoded as a gray value. Brighter points have a larger value of Gaussian curvature, while darker points have a smaller value. Fig.6 shows the result when rotation in the vertical direction is 0 degrees and -30 degrees in the horizontal direction. Curvature has similar values at corresponding points in the different poses. The results are qualitatively correct except in regions of cast shadow (or dirty regions), and the relative magnitude of Gaussian curvature is indeed recovered without using a distinct calibration object.
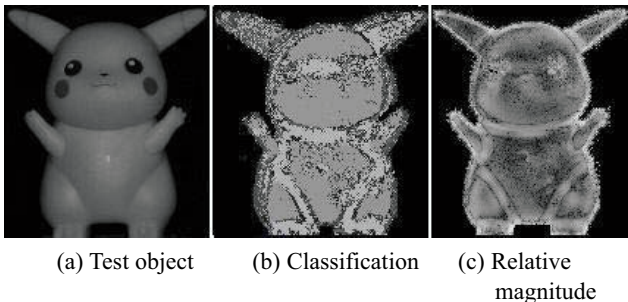

(a) Test object   (b) Classification   (c) Relative magnitude

Figure 5. Results for test object

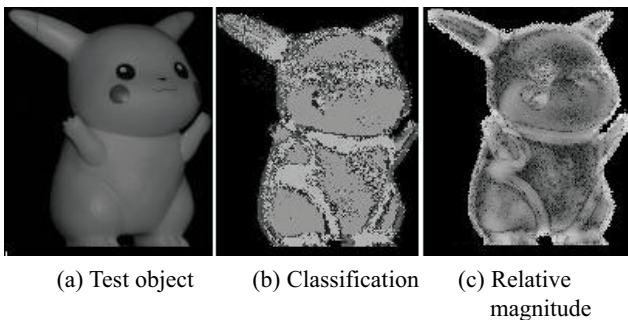(a) Test object   (b) Classification   (c) Relative magnitude

Figure 6. Results for test object

Figure 7. Surface classification

4.3. Effect of the number of light sources

Fig. 8 shows the relative magnitude of Gaussian curvature to compare the four light source case (left) with a three light source case (middle). The right image shows one of the input images. Improvement is observed in the four light source case. More light sources give a more robust result.
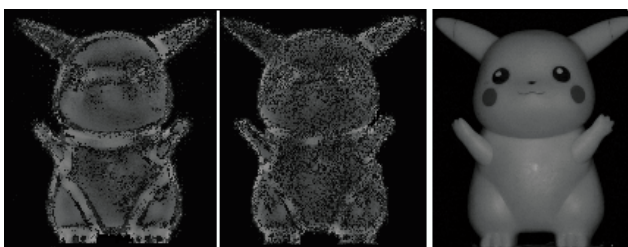

Figure 8. Results for comparison

5. Conclusion

This paper demonstrates a new method to recover the relative magnitude of Gaussian curvature at each visible point on a test object without using a separate calibration object. Instead, two degree of freedom rotation of the test object is used in self-calibration. With four input images, non uniform albedo is allowed since the effect of albedo is removed in neural network learning. Training data are obtained from the position of a marker point during rotation. The area surrounding each mapped point encodes the relative magnitude of the Gaussian curvature. The implementation described uses four light sources. Experiments are shown for a real object.

The method fails for points in cast shadow. Dealing with cast shadow and simplification of the implementation remain as future work

References

[1] R. J. Woodham, "Gradient and curvature from the photometric stereo method, including local confidence estimation," Journal of the Optical Society of America, A, Vol.11, pp.3050–3068, 1994.

[2] Y. Iwahori, R. J. Woodham, and A. Bagheri, "Principal components analysis and neural network implementation of photometric stereo," in Proc. IEEE Workshop on Physics-Based Modeling in Computer Vision, pp.117–125, June 1995.

[3] Y. Iwahori, R. J. Woodham, M. Ozaki, H. Tanaka, and N. Ishii, "Neural Network Photometric Stereo with a Nearby Rotational Moving light Source" IEICE Transactions on Information and Systems, Vol.E80-D, No.9, pp. 948–957, 1997.

[4] E. Angelopoulou and L.B. Wolf, "Sign of Gaussian Curvature from Curve Orientation in Photometric Space" in IEEE Trans. on PAMI, Vol.20, No.10, pp.1056-1066, Oct, 1998.

[5] T. Okatani and K. Deguchi, "Determination of Sign of Gaussian Curvature of Surface from Photometric Data" in Trans. of IPSJ, Vol.39, No.5, pp.1965-1972, Jun 1998.

[6] Y. Iwahori, S. Fukui, R. J. Woodham, A. Iwata, "Classification of Surface Curvature from Shading Images Using Neural Network," IEICE Trans. on Information and Systems, Vol.E81-D, No.8, pp.889-900, 1998.

[7] Yuji Iwahori, Shinji Fukui, Chie Fujitani, Yoshinori Adachi and Robert J. Woodham, "Relative Magnitude of Gaussian Curvature from Shading Images Using Neural Network, " KES2005, Knowledge-Based Intelligent Information & Engineering Systems, LNAI 3681, pp.813-819, 2005